Tuning the Hydrogenation Selectivity of an Unsaturated Aldehyde via Single-Atom Alloy Catalysts

Hio Tong Ngan[1], Philippe Sautet[1,2,3*]

[1]Department of Chemical and Biomolecular Engineering, University of California, Los Angeles, California 90095, United States

[2]Department of Chemistry and Biochemistry, University of California, Los Angeles, California 90095, United States

[3]California NanoSystems Institute, University of California, Los Angeles, CA 90095, USA

corresponding author: sautet@ucla.edu

Abstract

Selective hydrogenation of α,β-unsaturated aldehydes to produce unsaturated alcohols remains a challenge in catalysis. Here we explore, on the basis of first-principles simulations, single-atom alloy (SAA) catalysts on copper as a class of catalytic materials to enhance the selectivity for C=O bond hydrogenation in unsaturated aldehydes by controlling the binding strength of the C=C and C=O bonds. We show that on SAA of early-transition metals such as Ti, Zr, and Hf, the C=O binding mode of acrolein is favored, but the strong binding renders subsequent hydrogenation and desorption impossible. On SAA of late-transition metals, on the other hand, the C=C binding mode is favored and C=C bond hydrogenation follows, resulting in the production of undesired saturated aldehydes. Mid-transition metals (Cr, Mn) in Cu(111) appear as the optimal systems, since they favor acrolein adsorption via the C=O bond but with a moderate binding strength, compatible with catalysis. Additionally, acrolein migration from the C=O to the C=C binding mode, which would open the low energy path for C=C bond hydrogenation, is prevented by a large barrier for this process. SAA of Cr in Cu appears as an optimal candidate, and kinetic simulations show that the selectivity for propenol formation is controlled by preventing the acrolein migration from the more stable C=O to the less stable C=C binding mode, subsequent H-migration, and by the O-H bond formation from the mono-hydrogenated intermediate. Dilute alloy catalysts therefore enable tuning the binding strength of intermediates and transition states, opening a control of catalytic activity and selectivity.

Introduction

Selective hydrogenation of α,β-unsaturated aldehydes to produce unsaturated alcohols is an essential process in the fine chemicals and pharmaceutical industries.[1] However, this reaction remains a challenge in catalysis as thermodynamically, it is easier (by about 35 kJ/mol) to hydrogenate the C=C bond of the unsaturated aldehydes, forming the saturated aldehydes, than to hydrogenate the C=O bond.[2] Hence, selective hydrogenation of the C=O bond to produce unsaturated alcohols is a kinetically controlled process, and requires a specific catalyst for attainment. Common active hydrogenation catalysts such as the Pt-group metals, however, have been previously shown to favor the C=C bond hydrogenation over the C=O bond hydrogenation.[3–5] Other studies by Laref et al. and Loffreda et al. demonstrate that the unsaturated alcohol could be formed by hydrogenation of acrolein on the Pt(111) surface, but that desorption of this product is difficult, therefore favoring the gas phase formation of saturated aldehyde.[6,7] Although some alloy catalysts, such as $Pd_{0.001}Ag_{0.999}/SiO_2$, $Sn_{0.32}Rh_{0.68}/SiO_2$, $Pt_{0.005}Cu_{0.995}$/SBA-15, and $Ir_{0.13}Au_{0.87}/TiO_2$ etc., have been reported to be more selective and reactive than their monometallic counterparts in the literature, they either still possess considerably low selectivity values or demonstrate efficacy exclusively for larger and bulkier unsaturated aldehydes.[8–12] Therefore, there exists a pressing necessity to resolve the selectivity issue through the development of innovative catalysts, especially for small unsaturated aldehydes which do not benefit from the destabilization of the C=C bond by the substituents.

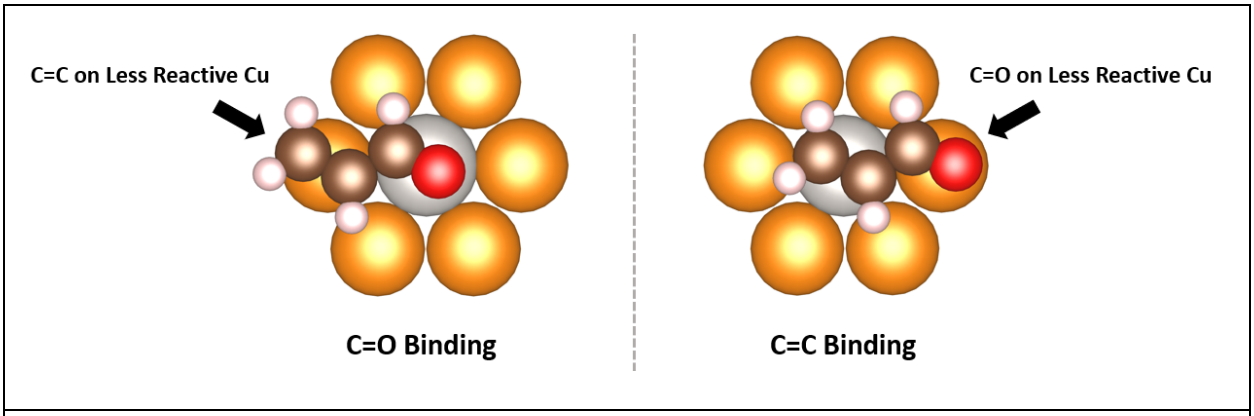

Figure 1. Schematic diagram demonstrating the C=O and C=C binding modes of acrolein on a single-atom alloy catalyst.

Single-atom alloys, which are formed by dispersing a small amount of active elements in less active metals (e.g. Au, Ag, and Cu), could be a promising class of catalytic materials to enhance the selectivity for C=O bond hydrogenation in unsaturated aldehydes.[13–18] The concept is that in addition to H_2 activation, a well-chosen dopant element could favor the C=O binding mode and its subsequent hydrogenation, while the C=C bond will sit on a rather less reactive part of the surface (Figure 1 left). The binding strength of the C=C and C=O bonds on the dopant element depends largely on their interaction with the dopant's d-states. Typically, when an active dopant is diluted in an inert metal host, it tends to have d-states narrow in energy due to the weak orbital mixing between the two elements.[19,20] By diluting early-, mid- and late-transition metals in noble metals, the relative energy position of the dopant's d-states could be adjusted, and the optimal interaction between the two functional groups in unsaturated aldehydes and the dopant atoms could be achieved.

Single-atom alloy catalysts made of dilute Pd in Au have been shown to effectively increase the semi-hydrogenation selectivity of alkynes, and to provide different rate and selectivity controlling steps compared to monometallic catalysts due to geometric constraint.[21,22] Dilute Pt in Cu catalysts were shown to selectively promote the hydrogenation of C=O bonds in unsaturated aldehydes, however surface spectroscopy showed that the surface is covered by a thin Cu oxide layer so that the origin of the observed selectivity is not fully understood.[10] Monometallic Ag has been shown to possess high selectivity for allyl alcohol formation, although difficult H_2 activation on it often leads to low reaction activity. Highly dilute Pd in Ag catalytic nanoparticles on SiO_2 (~1 Pd for 800 Ag), however, provided a selectivity for acrolein hydrogenation to propenol (31%) close to that on Ag nanoparticles, but with an improvement in the activity.[11] Pd on Ag(111) SA alloys were further studied for the same reaction of acrolein hydrogenation with temperature programmed desorption.[23] Compared to Ag(111), adding Pd SAs increased the conversion of acrolein but decreased the selectivity to propenol. In a different investigation of selective hydrogenation on alloys, the addition of Sn to Pt was found to significantly enhance the selectivity for allyl alcohol formation from 1.6 to 27.5 %.[3] Using density functional theory, some of us suggested that the charge transfer from Sn (to form Sn^+) to Pt favors the binding of the acrolein molecule via its

aldehyde functionality, which could explain the improved selectivity observed if this adsorption configuration leads to C=O bond hydrogenation.[24]

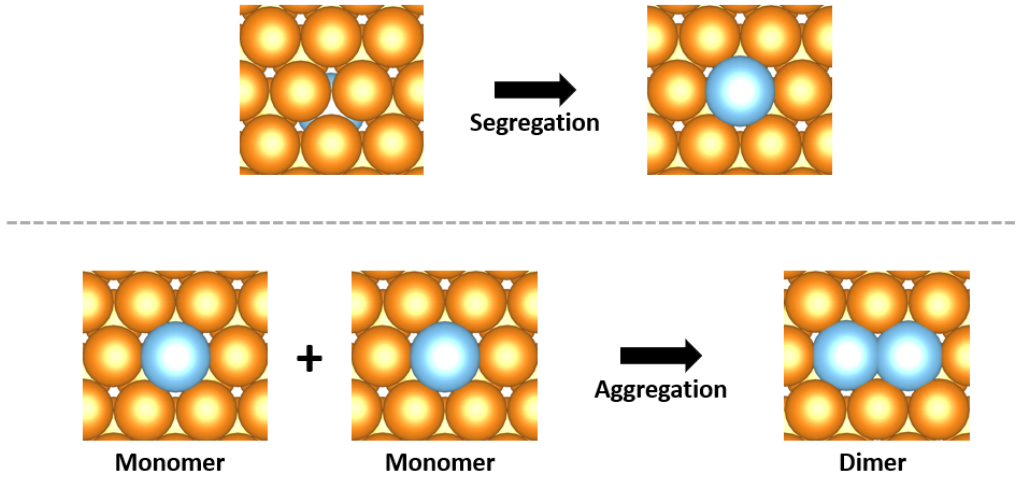

Figure 2. Schematic diagram showing the processes of segregation and aggregation of dopants in dilute alloy catalysts. Segregation is to bring the dopant atom from the subsurface layer to the surface layer, and aggregation is to bring two isolated surface dopant atoms (monomers) together to form a dimer.

Although the class of SA alloy catalysts could offer an improved selectivity, concern is often raised regarding the dopant's segregation and aggregation for optimal catalytic performance (Figure 2). Ideally, active dopants should stay in the surface layer (favorable surface segregation) as isolated atoms in the metal host, avoiding aggregation into larger metal ensembles at the surface. However, alloy combinations that exhibit slight tendencies towards anti-segregation and aggregation can still be utilized, provided they undergo adequate pre-treatment. For example, pre-treatment under CO or O_2 pressures prior to reactions can enable one to disperse and position the dopant atoms in the surface layer in a metastable situation.[25] A previous computational study proposed that dilute Fe-in-Au alloy catalyst could be a promising candidate for selective hydrogenation of unsaturated aldehydes, and it was shown that the calculated product selectivity is consistent with the crotonaldehyde initial adsorption configurations in cases that the authors have tested.[17] Using this conclusion as a starting point, other alloy combinations are explored in detail in the present work, and combination with kinetic simulations enable us to excavate potential catalysts for this reaction.

Herein, trends in early-, mid-, and late-transition metals dispersed in the less reactive metal Cu were investigated using theoretical modeling to offer insights into the rational design of novel catalysts for selective hydrogenation of unsaturated aldehydes into unsaturated alcohols. Acrolein, being the smallest possible unsaturated aldehyde, was employed as the model reactant for this purpose. Selectivity to unsaturated alcohols is expected to be higher for larger unsaturated aldehydes with a functional group attached to the C=C bond (e.g. crotonaldehyde and cinnamaldehyde etc.) than for acrolein as the extra functional group could destabilize the transition states for C=C bond hydrogenation. In addition, the presence of the extra substituents is also anticipated to reduce the binding strength of the unsaturated alcohols formed and to facilitate

desorption, as demonstrated by a former study on Pt(111) by Laref et al.[7] Hence, if acrolein is selectively hydrogenated on a specific catalyst and could desorb with ease, the same should also apply to other larger unsaturated aldehydes. Nevertheless, substituent effect is not the only factor controlling selectivity as will be discussed. In this study, it is demonstrated that on SAA of early-transition metals such as Ti, Zr, and Hf, the C=O binding mode of acrolein (and subsequent mono-hydrogenated intermediate) is much more stable when compared with the C=C binding mode. However, the binding is too strong such that subsequent hydrogenation and desorption steps are highly endergonic in nature. On SAA of late-transition metals, on the other hand, the C=C binding mode of acrolein and subsequent C=C bond hydrogenation is more favorable, resulting in the production of the undesired saturated aldehydes. Mid-transition metals (Cr, Mn) in Cu(111) are the most promising choices as they offer moderate binding strength and facilitate acrolein adsorption via the C=O bond. Particularly, the barrier preventing acrolein migration from its more stable configuration in the C=O binding mode to the less stable but more reactive and unselective C=C binding mode, together with the barrier for H-migration to that C=C binding acrolein, help enhance the selectivity. This enhancement occurs because these transition states (acrolein diffusion and H-migration) exhibit a comparable free energy to the rate-limiting transition state in the C=O hydrogenation pathway. Together, these results show that by carefully tuning the interaction between the catalyst surface and the two functional groups in acrolein, single-atom alloy catalysts could open up new opportunities for selective hydrogenation of α,β-unsaturated aldehydes.

Methods

DFT Calculations: All density functional theory (DFT) calculations were performed using the Vienna ab initio simulation package (VASP).[26,27] The (111) surfaces of the various bimetallic catalysts were modeled using a four-layer slab and a (3 × 3) unit cell, and a Monkhorst-Pack[28] generated 5 × 5 × 1 K-points grid was employed for this unit cell size. Increasing the K-points grid further to 7 × 7 × 1 is demonstrated to have negligible impact ($\Delta E < 0.02$ eV) on the total energy obtained for the $CuTi_1$ slab, let alone the adsorption energies in which the differences could be cancelled out in the calculations. During structural optimization, the bottom two layers of the slab were constrained in the bulk Cu position, while the upper two layers and the surface adsorbates were allowed to relax until the force convergence threshold of 0.02 eV/Å was reached. A plane wave basis set with a cutoff energy of 450 eV, the dDsC-dispersion-corrected PBE functional were used and spin polarization was included for all calculations.[29,30] The second order Methfessel-Paxton smearing method with the width of smearing set to 0.2 eV was also employed for these calculations.[31] Standard PAW pseudopotentials were utilized for all elements except for the early-transition metals Ti, Zr, and Hf. For these early-transition metals, the versions 'Ti_sv' with 12 valence electrons, 'Zr_sv' with 12 valence electrons, and 'Hf_pv' with 10 valence electrons were used instead.[32,33] Transition states were located using both the climbing image nudged elastic band (CI-NEB) and the dimer methods.[34–36] Crystal Orbital Hamilton Populations (COHP) analysis was made feasible using the Local Orbital Basis Suite Towards Electronic Structure Reconstruction (LOBSTER).[37] All structural configurations reported in this study are visualized using VESTA.[38]

The segregation energy reported in this study is defined as the energy gain/loss to bring a dopant atom from the subsurface layer of the metal slab to the surface layer, and hence is calculated as:

$$E_{seg} = E_{surf} - E_{subsurf} \quad (1)$$

where E_{seg} is the segregation energy, E_{surf} is the DFT energy of the metal slab when the dopant is in the surface layer, and $E_{subsurf}$ is the DFT energy when the dopant is in the subsurface layer.

Aggregation energy, on the other hand, is defined as the energy gain/loss to bring two separated surface dopant atoms together, and is calculated as:

$$E_{agg} = E_{dimer} + E_{Cu} - 2 * E_{monomer} \quad (2)$$

where E_{agg} is the aggregation energy, E_{dimer} is the DFT energy of the metal slab when two surface dopant atoms are brought together, E_{Cu} is the energy of a pure Cu slab for balancing the number of atoms, and $E_{monomer}$ is the energy when there is only one dopant atom in the surface layer of the slab.

For simplicity, free energy calculations only consider the translational and rotational entropies of the gaseous species. Zero-point energies (ZPEs) and vibrational contributions of the entropies of all species were neglected.

Microkinetic Modeling: Microkinetic modeling was performed using the DFT energies as input parameters to study the reaction selectivity. In this modeling, the rate constants for adsorption ($k_{ads,i}$)/desorption ($k_{des,i}$) and surface reaction steps (k_j) were computed using the collision theory (Equations 3a and 3b) and transition state theory (Equation 4), respectively:[39]

$$k_{ads,i} = \frac{A_{st}}{\sqrt{2\pi m_i k_B T}} \quad (3a)$$

$$k_{des,i} = k_{ads,i} P^o exp\left(\frac{\Delta G^o_{ads,i}}{k_B T}\right) \quad (3b)$$

$$k_j = \frac{k_B T}{h} exp\left(-\frac{\Delta H^{\ddagger,o}}{k_B T}\right) exp\left(\frac{\Delta S^{\ddagger,o}}{k_B}\right) \quad (4)$$

where A_{st} is the effective area of the adsorption site, m_i is the mass of the adsorbing species i, k_B is the Boltzmann's constant, T is the temperature, P^o is the standard state pressure, $\Delta G^o_{ads,i}$ is the adsorption free energy of species i under standard state pressure, h is the Planck's constant, and $\Delta H^{\ddagger,o}$ and $\Delta S^{\ddagger,o}$ are respectively the standard-state enthalpy and entropy differences between the initial state and the transition state in elementary step j.

Surface species coverages were used to calculate the acrolein consumption and propenol production rates, as manifested in their elementary step rate equations. To solve the surface species coverages, a set of ordinary differential equations (O.D.E.s) were constructed based on the reaction network considered (See Table S1 and Equation 5):

$$\frac{d\theta_i}{dt} = \sum_j \nu_{ij} r_j \quad (5)$$

where θ_i is the surface coverage of species i, t is time, ν_{ij} is the stoichiometric coefficient of species i in step j, and r_j is the reaction rate of elementary step j. These O.D.E.s were solved by assuming the surface to be initially bare. Once the surface species coverages and hence the steady-state reaction rates were obtained, the selectivity (S) for propenol formation was calculated as follows:

$$S = \frac{Propenol\ Formation\ Rate}{Acrolein\ Consumption\ Rate} \quad (6)$$

Degree of selectivity control (DSC) analysis[40] was also carried out to identify the elementary steps that have a significant impact on the reaction selectivity. DSC was calculated as:

$$DSC = \left(\frac{\partial \ln S}{\partial \left(-\frac{G_i^0}{k_B T} \right)} \right)_{G_{j \neq i}^0} \quad (7)$$

where G_i^0 is the standard-state free energy of species i. The partial derivative in equation 7 is taken such that the standard-state free energies of all other species are kept constant. The degree of rate control (DRC) was calculated in a similar manner, except that selectivity should be replaced by acrolein consumption rate in Equation 7. By definition, a positive DRC/DSC value indicates that the rate/selectivity would be enhanced if the standard-state free energy of species i is lowered, and vice versa.

Results

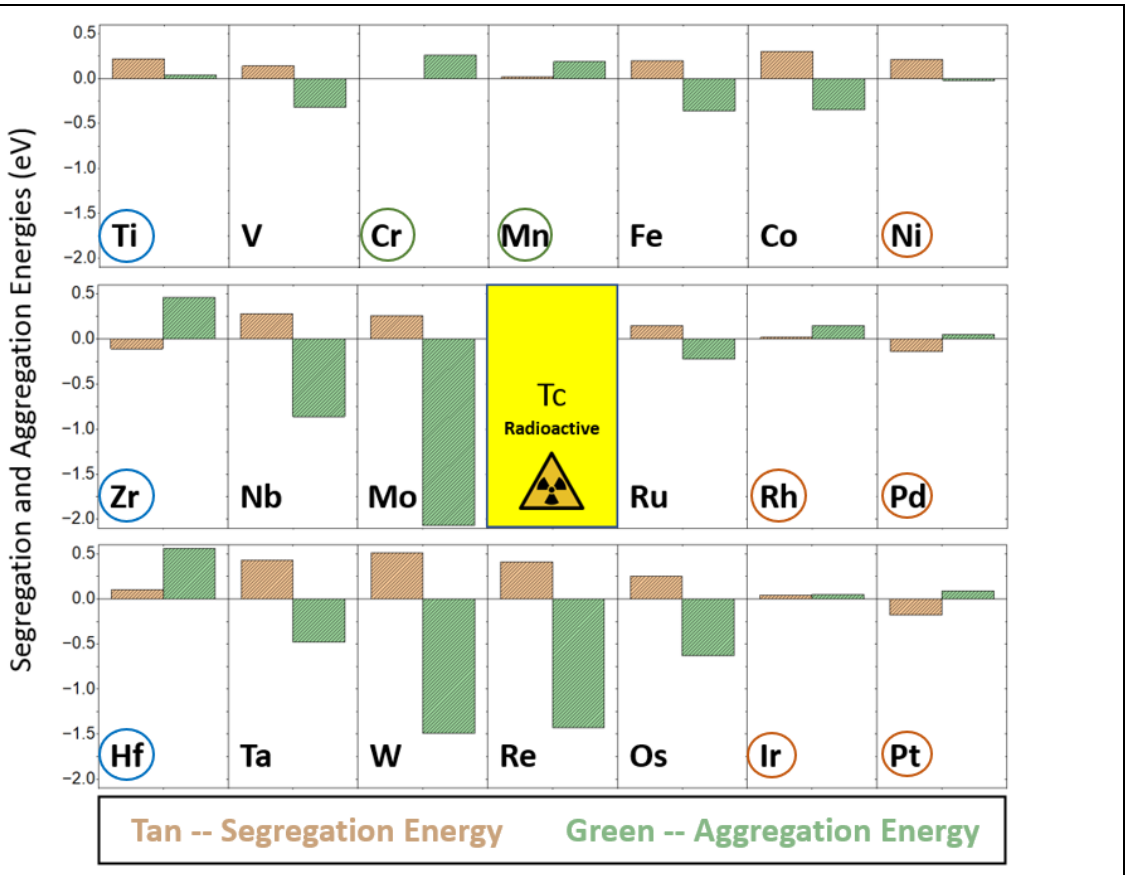

Figure 3. Segregation (tan) and aggregation (green) energies of various transition metals in Cu(111). Negative segregation energies indicate that segregation is favorable while positive aggregation energies imply that aggregation is unfavorable.

In a single-atom alloy catalyst, the active dopant should be present in the surface layer of the less reactive metal host as an isolated atom. To figure out if such catalysts can be made experimentally, segregation and aggregation energies were evaluated for all transition metals of group 4 to 10 (except for Tc) in the Cu host (Figure 3). Ideally, the segregation and aggregation energies should be negative and positive, respectively, for such single-atom alloy catalysts to be stable. Nevertheless, catalysts with a slightly positive segregation energy are still tolerable as they can be pretreated prior to reactions to position the active metal in the surface layer and function as metastable states.[25] Out of the various alloy combinations, early-transition metals Ti, Zr, and Hf, mid-transition metals Cr and Mn, and late-transition metals Rh, Ir, Ni, Pd, and Pt are found to have acceptable segregation and aggregation energies and therefore to be realizable. Ti in Cu(111) is the one that has the most positive segregation energy value in these 10 alloy candidates, but its magnitude is only 0.22 eV, which is small enough for pretreatment to bring it up to the surface layer where it could stay during the course of the reaction. In particular, Ti has been previously shown to exist as isolated atoms in the Cu(111) surface in experiment.[41] Additionally, unlike other

alloy combinations, these 10 candidates do not have a strong tendency to aggregate, making them viable to be created as single-atom alloys experimentally.

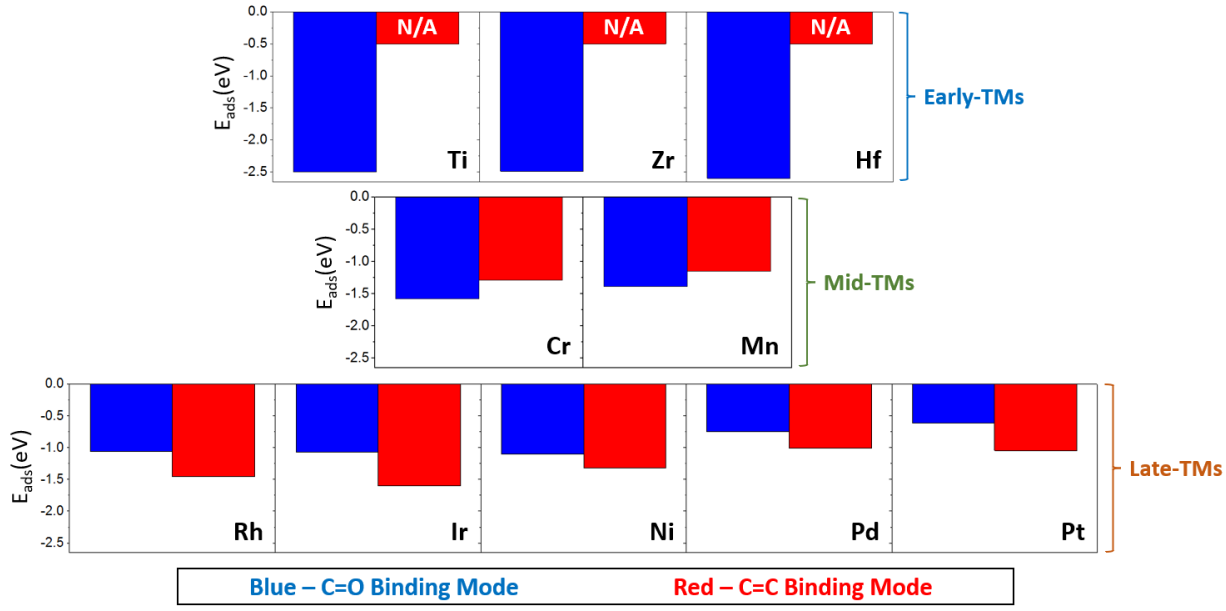

Figure 4. Adsorption electronic energies of acrolein on early-, mid-, and late-transition metals in Cu(111) with the C=O (blue, C=O binding mode) and C=C (red, C=C binding mode) bonds on top of the dopant atom. No adsorption energy is reported for the C=C binding mode on early-transition metals as this configuration is not a metastable state on them and transforms into the C=O binding mode.

Energies of adsorption for acrolein, locating the C=O or the C=C bond on the dopant, were evaluated on the 10 previously mentioned alloy candidates as a preliminary assessment to figure out if they are capable of selectively forming propenol (Figure 4). A former study proposed that this initial adsorption configuration of the unsaturated aldehydes would determine the reaction selectivity.[17] In other words, if C=O binding mode is preferred over C=C binding mode, subsequent hydrogenation of the C=O bond would also be more favorable. Early-transition metal SAAs of Ti, Zr, and Hf in Cu(111) demonstrate a very strong tendency to adsorb acrolein via its O atom in the C=O bond (C=O binding mode), while the remaining part of the molecule sits on the Cu surface. Indeed, these early-transition metals are so oxophilic that the adsorption energies by the O atom are more negative than -2.45 eV, and that no stable C=C binding mode was observed. Mid-transition metal SAAs of Cr and Mn in Cu(111) also favor the C=O binding mode over the C=C binding mode, by 0.29 eV and 0.24 eV respectively. Similar to the early-transition metals, it is mainly the O atom in the C=O bond that interacts with Cr and Mn for the C=O binding mode, and the rest of the acrolein molecule lies flat on the surface. In the case of the C=C binding mode, both C atoms in the C=C bond participate in the interaction with the dopants based on the similar interatomic distances observed. The binding strength of acrolein on these mid-transition metals, however, is much weaker than that on the early-transition metals, regardless of the binding modes. Lastly, late-transition metals Rh, Ir, Ni, Pd, and Pt do not favor the C=O binding mode. As a matter

of fact, the C=C binding mode on them is 0.22 to 0.53 eV more stable than the C=O binding mode. This preliminary result suggests that early- and mid-transition metals in Cu(111) could be candidates to selectively hydrogenate acrolein to propenol, but late-transition metals would not. Nevertheless, further investigation is required in order to substantiate this assertion.

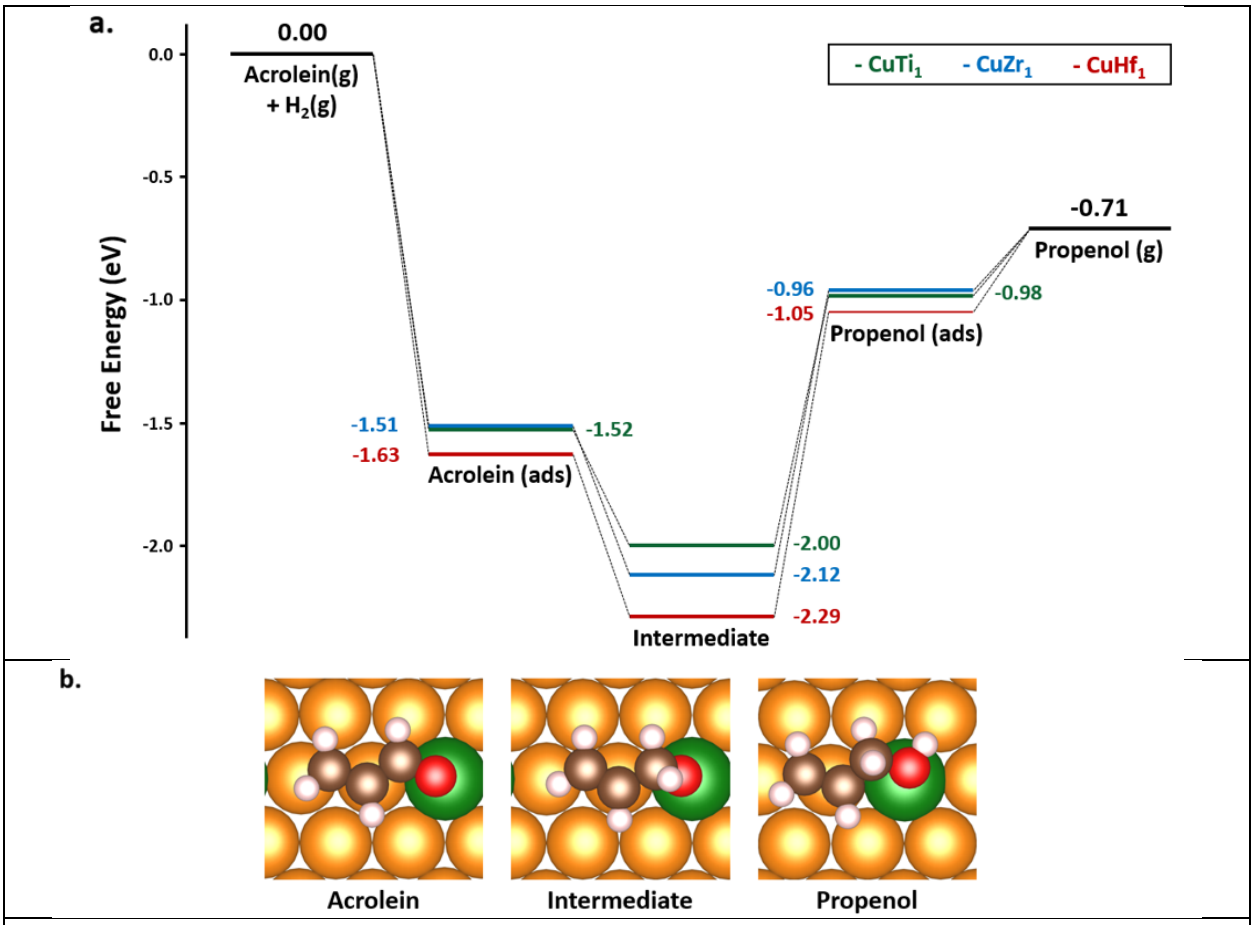

Figure 5. (a) Free energy profile for acrolein hydrogenation on $CuTi_1$ (green), $CuZr_1$ (blue), and $CuHf_1$ (red). (b) Corresponding reaction configurations on $CuTi_1$. Transition states are omitted in this study for simplicity. Reaction conditions are: T = 375 K, P(Acrolein) = 0.1 bar, $P(H_2)$ = 300 bar, and P(Propenol) = P(Propanal) = 0.01 bar.

Early-transition metal single-atom alloys were first studied in detail for their enticing ability to only bind an acrolein molecule in the C=O binding mode. A simplified free energy profile was constructed to compare the energy differences between each intermediate along the hydrogenation pathway for the three early-transition metals Ti, Zr and Hf (Figure 5; Figure S1 for reaction configurations on $CuZr_1$ and $CuHf_1$). It is shown that acrolein binds to these surfaces very strongly, the adsorption free energies being -1.52, -1.51, and -1.63 eV for $CuTi_1$, $CuZr_1$, and $CuHf_1$, respectively. The feature of strong binding is preserved for the mono-hydrogenated intermediates, which are formed by hydrogenating the C atom in the C=O bond, and these states lie even lower in the free energy profile (G = -2.00 eV to -2.29 eV). The strong binding of acrolein and intermediates on the catalysts appears to be very alluring as it is anticipated to effectively lower

down the activation barriers for the C-H bond-formation towards the intermediate. However, this strong binding renders all the formation of adsorbed propenol highly endergonic (by 1.02 to 1.24 eV), and also makes its desorption unfavorable under the studied conditions, by at least 0.25 eV. Hence, instead of being able to readily and selectively hydrogenate acrolein, early-transition metals in Cu(111) are likely to be poisoned by the mono-hydrogenated intermediates and become unreactive due to the unfavorable thermodynamics along the second half of the pathway. For selective hydrogenation, the C=O bond binding should be favored, but its adsorption should not be too strong, following the Sabatier principle.

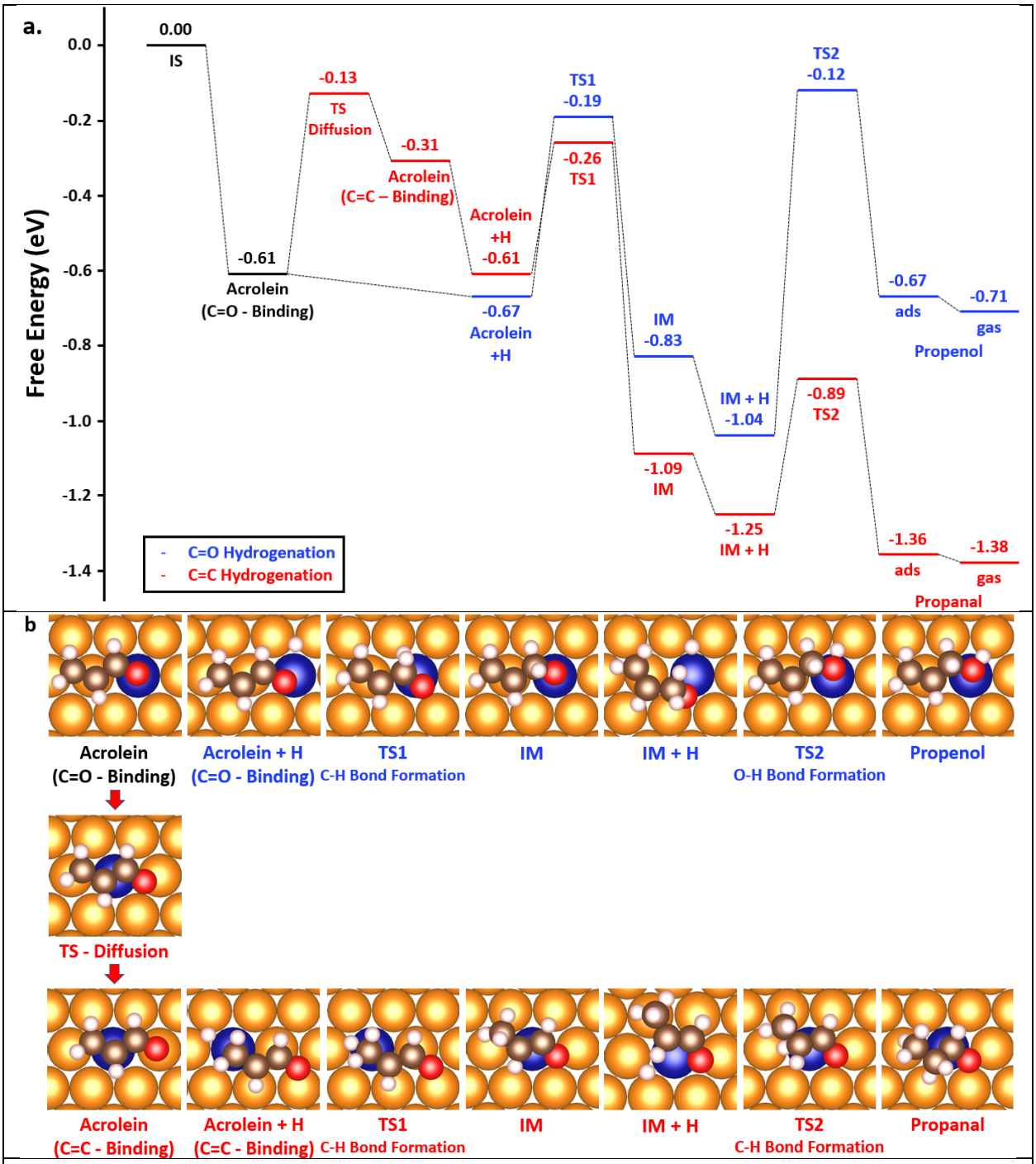

Figure 6. (a) Free energy profile for hydrogenation of the C=O bond (blue) and C=C bond (red) in acrolein on $CuCr_1$ and (b) Configurations of the corresponding reaction intermediates and transition states along the energy profile. Reaction conditions are T = 375 K, P(Acrolein) = 0.1 bar, $P(H_2)$ = 300 bar, P(Propanal) = 0.01 bar, and P(Propenol) = 0.01 bar.

Mid-transition metals in Cu(111) might open up new opportunities for selective acrolein hydrogenation as they favor the C=O binding mode, and the binding strength is moderate. A detailed study of the reaction mechanism on $CuCr_1$ was first carried out to ascertain the veracity

of that assertion (Figure 6 and Figure S2). The free energy profile for this reaction begins with the adsorption of acrolein in its most stable configuration, i.e. the C=O binding mode on the Cr dopant. The hydrogenation pathway of the C=O bond (Figure 6, blue pathway) then proceeds by drawing one H atom to its adsorption site (blue "Acrolein + H"), followed by the transition state for C-H bond formation (blue "TS1") to produce the mono-hydrogenated intermediate (blue "IM"). Once the mono-hydrogenated intermediate is formed, a second H atom is drawn to its adsorption site before going through the transition state for O-H bond formation (blue "TS2") and producing the desired product propenol. Similarly, the C=C bond hydrogenation pathway (Figure 6, red pathway) follows the same pattern. However, the acrolein molecule needs to first transform from the more stable C=O binding mode to the less stable C=C binding mode prior to the reaction, and the transition state for this transformation is labelled as "TS – Diffusion".

It is worth noting that the H atoms that are drawn to the reactant adsorption site are generated on a second active site or on the Cu(111) surface (which has been previously shown to be capable of performing H_2 activation) due to the constraint of the small ensemble size.[42] This H_2 activation process on a second $CuCr_1$ active site (Figure S2) begins with the molecular adsorption, which is slightly exergonic in nature (ΔG = -0.04 eV) under such high pressure. Adsorbed H_2 molecules subsequently split into two separated H atoms by going through the transition state for dissociation (TS-Dis in Figure S2), and the obtained activation barrier is moderate ($\Delta G^{\ddagger}$ = 0.38 eV). Following the dissociation, the separated H atoms could migrate to the reactant adsorption site via the Cu surface. The activation barrier associated with the migration of the H atoms to the Cu domain is similar to that for H_2 dissociation, with the value being 0.37 eV. With these small activation barriers ($\Delta G^{\ddagger}$ = 0.37 – 0.38 eV), H_2 activation and H atom migration by spill-over on the Cu could take place with ease on the $CuCr_1$ surface for acrolein hydrogenation. Eventually, it should be highlighted that H_2 activation on the Cu(111) surface encounters a somewhat higher barrier, with the value being 0.56 eV under the same studied conditions. Nevertheless, this pathway can still serve as an additional way to supply H atoms for the hydrogenation reaction.

The free energy profile for acrolein hydrogenation on $CuCr_1$ indicates that the initial adsorption of acrolein is moderate, with the free energy change being -0.61 eV for the C=O binding mode which mainly occurs through a O-Cr interaction (Figure 6). Adsorption by the C=C bond is possible but is 0.3 eV less stable, which would correspond to a Boltzmann population of ~10^{-4}. However, this C=C binding mode is more prone to hydrogenation. First, hydrogen co-adsorption with the C=C binding mode is thermodynamically easier than that with the C=O binding mode, which reduces the stability difference between the two co-adsorbed states to 0.06 eV. Second, the first hydrogenation at the C atom is easier for C=C binding mode with a transition state free energy of -0.26 eV, versus -0.19 eV for the C=O binding mode. It should be highlighted that hydrogenating the C atom in the C=O bond as the first step is more favorable than hydrogenating the O atom due to the oxophilic nature of Cr. Once the O atom is hydrogenated, the interaction between it and the active dopant will be weakened. This claim is justified by the higher adsorption energy of the mono-hydrogenated intermediate $CH_2CHCHOH$ than that of CH_2CHCH_2O, with the difference being 0.29 eV. In addition, previous study finds that in acetaldehyde hydrogenation on $CuNi_1$, which is a less oxophilic element, the transition state energy for C-hydrogenation in the C=O bond is 0.68 eV lower than that for O-hydrogenation.[43] This difference is expected to be even larger on

the more oxophilic Cr. Using this result as an analogy, the transition state for hydrogenating the O atom in the C=O bond of acrolein would also lie much higher in the energy profile than both the blue "TS1" and "TS2" in Figure 6. Hence, this pathway is likely to be less favorable than the one detailed in this study.

Consistent with the transition states, the intermediate formed from hydrogenating the C=C bond (-1.09 eV) also lies lower in the free energy profile than that formed from C=O bond hydrogenation (-0.83 eV). The same also applies to the second transition states to hydrogenate the remaining O and C atoms as the transition state for the former is as high as -0.12 eV, while that for the latter is only -0.89 eV. The lower transition state energies seem to suggest that C=C bond hydrogenation is kinetically more favorable than C=O bond hydrogenation on $CuCr_1$. However, the diffusion transition state to transform acrolein from its more stable C=O binding configuration to the less stable C=C binding configuration also lies high in the energy profile. In fact, this transition state has a free energy value of -0.13 eV, which is very similar to the transition state for O-H bond formation (blue "TS2", G = -0.12 eV). This negligible difference indicates that selective hydrogenation of acrolein on $CuCr_1$ is still probable. In addition, there are transition states, although omitted for simplicity in Figure 6, to bring H in proximity to reactants, or intermediates, and form the co-adsorption states. H atoms are readily available at steady state on the Cu surface as will be discussed in the microkinetic modeling section, and the activation barrier to bring a H atom from the Cu surface to their adsorption sites is roughly 0.2 eV (Figure S2 from H(Cr,Cu) to TS-M). Adding this barrier to the free energy of acrolein in the C=C binding mode provides a transition state energy equal to -0.11 eV, which is very close to that of the diffusion TS. It is hence expected that C=C hydrogenation on $CuCr_1$ is not favored, and an improved selectivity could be expected from both the barrier for acrolein diffusion on the surface and the one to bring a H atom to the C=C bound acrolein molecule. The discussion on the free energy profile is however qualitative and a more comprehensive analysis will be provided by the following microkinetic modeling section. In the end, it is important to mention that the desorption of the two different products (propenol and propanal) is seen to be facile as demonstrated by the slightly exergonic nature of this process.

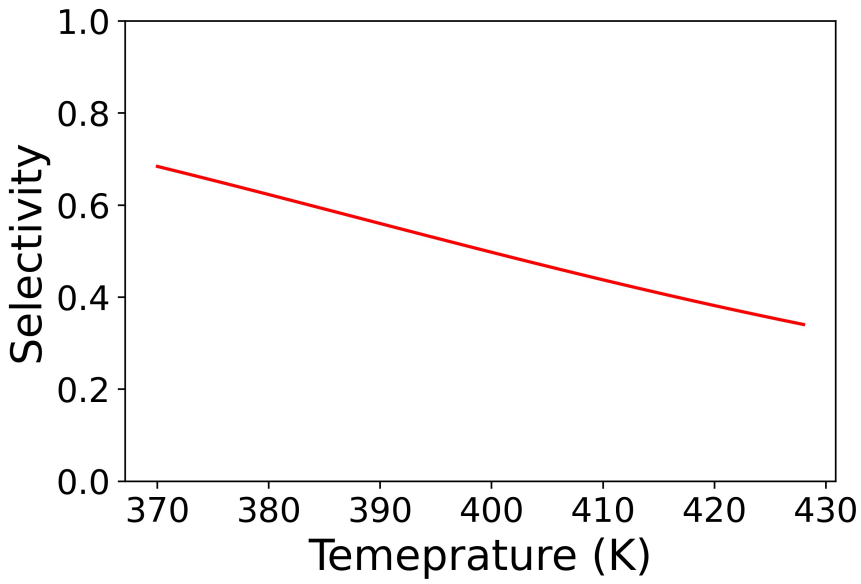

Figure 7. Selectivity for propenol formation on $CuCr_1$ as a function of temperature. Reaction conditions are P(Acrolein) = 0.1 bar, $P(H_2)$ = 300 bar, P(Propanal) = 0.01 bar, and P(Propenol) = 0.01 bar.

A microkinetic modeling, which takes into consideration the combined effect of intermediate and transition state free energies in the profile, was carried out to further assess the selectivity for propenol formation on $CuCr_1$ (Figure 7). Briefly, the elementary steps considered in this microkinetic modeling include H_2 activation on both the Cu(111) and SAA surfaces, and acrolein hydrogenation on the SAA surface. An H atom is drawn to the acrolein/mono-hydrogenated intermediate adsorption site from another SAA ensemble or from the Cu(111) surface before every bond-formation event (See Table S1). The microkinetic modeling result shows that at T = 370 K, the selectivity achieved for propenol production is nearly as high as 70 % (Figure 7). Additionally, degree of selectivity control (DSC; Figure S3) calculations from the kinetic modeling supports the free-energy-based analysis, in which the steps of acrolein diffusion and H-migration to the C=C binding molecule are demonstrated to be most negatively selectivity-determining, whereas the O-H bond formation step (blue 'TS2' in Figure 6) is positively selectivity-determining. It is noted that the selectivity here means selectivity towards propenol formation.

Despite the fact that higher temperature could improve the reaction reactivity, the desired selectivity diminishes to lower than 40 % when the temperature is above ~417 K. The inverse relationship between selectivity and temperature is also mirrored in the degree of rate control (DRC) analysis (Figure S4). Specifically, when the temperature is low (T = 375 K), the transition state for O-H bond formation (C=O hydrogenation pathway) is more rate-controlling than the ones for H-migration to the C=C binding acrolein and acrolein diffusion (C=C hydrogenation pathway), and the trend reverses when the temperature is higher (T = 475 K). This outcome suggests a shift in the predominant pathway of the reaction, transitioning from the C=O hydrogenation pathway to the C=C hydrogenation pathway, when the temperature is increased.

It is understood that elevated temperature stabilizes all gaseous species from an increased contribution of the entropy to the free energy, and therefore increasing the relative free energies of the surface transition states. Note that, however, the increased entropic contribution of gas phase acrolein affects all three selectivity-determining transition states equally, while that of gaseous H_2 does not have an equal impact on them. To be more specific, the diffusion transition state energy does not depend on the entropy of H_2 as this step does not need to involve any H atoms on the catalyst surface. The H-migration step to the C=C binding acrolein, on the other hand, requires the introduction of one H atom to the catalyst surface, and it suffers from entropic penalty associated with one-half of a gaseous H_2 molecule. This penalty becomes even more pronounced for the O-H bond formation step as this step involves two surface H atoms (one is found in the mono-hydrogenated intermediate and the other one is to be attached to the same intermediate), and the entropy in one gaseous H_2 molecule is lost to achieve this. Hence, at higher temperatures, there will be a greater increase in the free energy of the transition state for O-H bond formation, making the C=O hydrogenation pathway less favorable and the reaction selectivity lower. To counter this adverse effect of elevated temperature on selectivity, H_2 pressure, if possible, could be further increased to significantly bring the O-H bond formation transition state lower in energy, while having a smaller impact on the H-migration step and none on the diffusion step. Eventually, it should be mentioned that the large diffusion barrier can be seen as an additional and promising approach to control selectivity as its contribution does not depend on reaction conditions.

Although a high H_2 pressure could enhance the reaction selectivity, caution should be exercised regarding surface poisoning. Microkinetic modeling indicates that, in addition to the Cu surface, above 97 % of the dopant active sites on $CuCr_1$ are also covered by H atoms under the studied conditions (Figure S5). This observation is consistent with the energy profiles where the free energy of the "2H" state is -0.66 eV on $CuCr_1$ (Figure S2), and that of acrolein is only -0.61 eV (Figure 6). The same is also mirrored in the DRC study in which acrolein adsorption transition state is found to be the most rate-controlling (DRC ~= 1), as most of the active sites are occupied by H atoms, and the "2H" state is found to have a DRC value of ~ -1 (Figure S5). Despite the blocking of the active sites by the H atoms, a reasonable reaction rate of 0.03 s^{-1} at ~383 K is still observed, with the selectivity being ~60 %. Additionally, the dDsC-dispersion-corrected PBE functional is known to slightly overestimate the binding of H atoms.[44] The true coverage of H in experiments is expected to be lower. To further counter this site-blocking by the H atoms, the pressure of acrolein, along with the product partial pressures to maintain a ~10 % conversion, could be increased. Increasing the acrolein pressure would lower its adsorption free energy (making adsorption more stable) such that it could expel some of the H atoms due to competitive binding and enhance the reaction rate. Note that doing so would not affect the calculated selectivity as it does not change the relative energy difference among the selectivity-determining transition states. Before closing up, it should also be mentioned that reaction intermediates adsorbed on active dopants in single-atom alloys do not experience lateral interactions as they are inherently separated apart. Although the Cu surfaces are covered by H atoms, the lateral interaction between them and the reaction species on the dopants is negligible as they are all small in size. Hence, lateral interaction is not a concern in this study.

Besides the exchange-correlation functional, density functional theory (DFT) calculations are also prone to other errors originating from basis set limitations, treatment of core electrons, and numerical integration, which collectively impact the accuracy of the computed results. Generally, the magnitude of the error is assumed to be approximately ±0.1 eV. Two new sets of microkinetic modeling were hence carried out by increasing the energy of the transition state for acrolein diffusion and lowering the energy of the transition state for O-H bond formation by 0.1 eV to examine the selectivity change. These energy changes in the two transition states are demonstrated to further improve the selectivity for propenol formation (Figure S6). To be more specific, the selectivity is above 90 % when the reaction temperature is lower than ~385 K. Moreover, the hydrogenation reaction on $CuCr_1$ would remain selective (> 50%) towards propenol at elevated temperature (T ~= 477 K) such that the reaction rate could also be enhanced. Since the H-migration step is more selectivity-determining than these two steps, lowering the activation barrier for that specific process is predicted to exert an even stronger impact in enhancing the selectivity. Nevertheless, the intrinsic error in DFT calculations for each elementary step is not completely understood. One could only suggest that there is a high probability that $CuCr_1$ is capable of performing selective acrolein hydrogenation. The same should also apply to another mid-transition metal $CuMn_1$, on which the selectivity-determining transition states in both hydrogenation pathways ('TS – Diffusion' and blue 'TS1') have similar free energy values (Figure S7), despite the H-migration transition state is slightly lower (G ~= 0.00 eV) in this case and does not have a significant impact on the reaction selectivity (Figures S7 and S8).

The surface structure of the $CuCr_1$ and $CuMn_1$ catalysts might reconstruct by segregation under reaction conditions. The initial stability assessment of Figure 3 was performed on bare surfaces. When adsorbates are present, dopant segregation to the surface is further enhanced as the energy decrease by adsorption on the dopant is greater than both the energy increase by segregation and the small energy decrease when the adsorption is on Cu(111). Specifically, for $CuCr_1$, the adsorption free energy of two H atoms on the Cr_1 ensemble is -0.66 eV, while segregation is roughly quasi-thermoneutral and the adsorption free energy on Cu(111) is merely -0.36 eV. For $CuMn_1$, segregation (a quasi-thermoneutral process) is also expected to be facilitated by the adsorption of the H atoms, despite the coverage might be lower due to the smaller adsorption free energy of -0.55 eV (Figure S8). Although higher temperature would weaken the binding of adsorbates on the dopant, this high temperature regime is less of an interest due to the lower selectivity observed. If, on the other hand, one uses a higher pressure of reactants, their adsorption would become more favorable which would further promote dopant segregation. It is noted that the binding energy of adsorbates on dimers and even trimers is stronger than that on a monomer, which encourages the formation of larger surface aggregates in the presence of the adsorbate. Nevertheless, this scenario could be effectively suppressed by controlling the amount of dopants that are put into the less reactive metal host. Hence, by carefully managing reaction conditions and tuning dopant concentration, single-atom alloy surfaces are expected to remain unchanged throughout the reaction process.

It is worth noting that the high selectivity of $CuCr_1$ for propenol production is not attributed to easy bond-formation steps in the C=O hydrogenation pathway, but to the challenging steps of acrolein diffusion and H-migration. If one switches to a larger unsaturated aldehyde with a

substituent attached to the C=C bond, the selectivity for unsaturated alcohol formation might not be necessarily dependent on these non-bond-formation steps. It is expected that the presence of a large substituent at the C=C bond would prevent this part of the molecule from coming close to the catalyst surface. Additionally, its presence would also destabilize the transition states for C=C bond hydrogenation due to steric hindrance and facilitate the unsaturated alcohol desorption. As a matter of fact, our DFT calculations show that $AuFe_1$ might not selectively hydrogenate acrolein to produce propenol because the highest transition state in the C=O hydrogenation pathway (blue 'TS1') exceeds that in the C=C hydrogenation pathway (red 'TS1') by 0.12 eV (Figure S9). Additionally, C=C and C=O adsorption modes are very close in energy and acrolein diffusion from one to the other is easy and not rate-limiting. Nevertheless, the trend in the transition state energy difference between red 'TS1' and blue 'TS1' in Figure S9 can be effectively reversed if a methyl group is attached to the terminal C atom of acrolein (crotonaldehyde molecule), as shown by Spivey et al. in their study on $AuFe_1$.[17] In short, reaction selectivity is controlled by various factors, and the use of diffusion barrier, in addition to the commonly-known substituent effect, can be seen as a promising approach to enhance selectivity in the hydrogenation of unsaturated aldehydes.

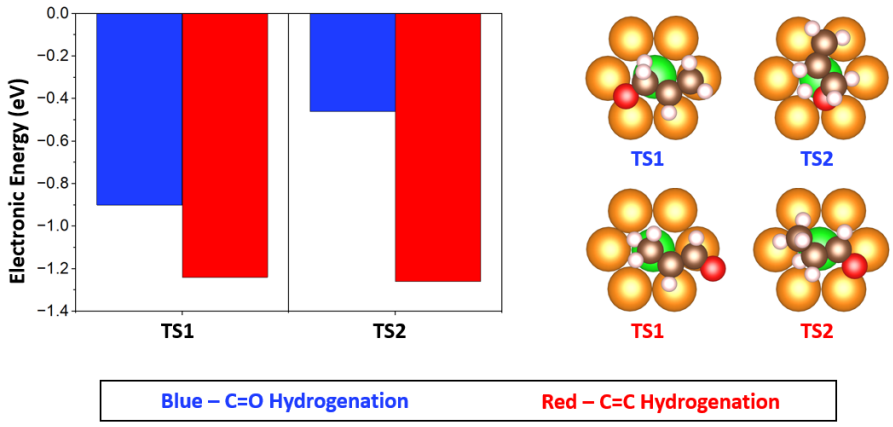

Figure 8. Electronic energies and the corresponding configurations of the transition states for C=O (blue) and C=C (red) hydrogenation on $CuNi_1$.

To eliminate the possibility of late-transition metals (which favor the C=C binding mode) being able to selectively hydrogenate the C=O bond in acrolein, the energies of the transition states for both hydrogenation pathways were computed on $CuNi_1$ (Figure 8). $CuNi_1$ was chosen among the five late-transition metals because it has the smallest adsorption energy difference (0.22 eV) between the two binding modes. Hence, Ni is the late-transition metal that could most possibly possess lower transition state energies for the C=O hydrogenation pathway than for the C=C hydrogenation pathway. Nevertheless, DFT calculations still show that the former pathway has much higher transition state energies (Figure 8). Specifically, the first transition state for C=O bond hydrogenation is 0.34 eV higher than that for C=C bond hydrogenation, and the difference in the second transition states is even as large as 1.20 eV. Hence, $CuNi_1$ is not capable of selectively hydrogenating the C=O bond in acrolein. The same conclusion could also be safely extended to other late-transition metals with greater adsorption energy differences between the two binding modes.

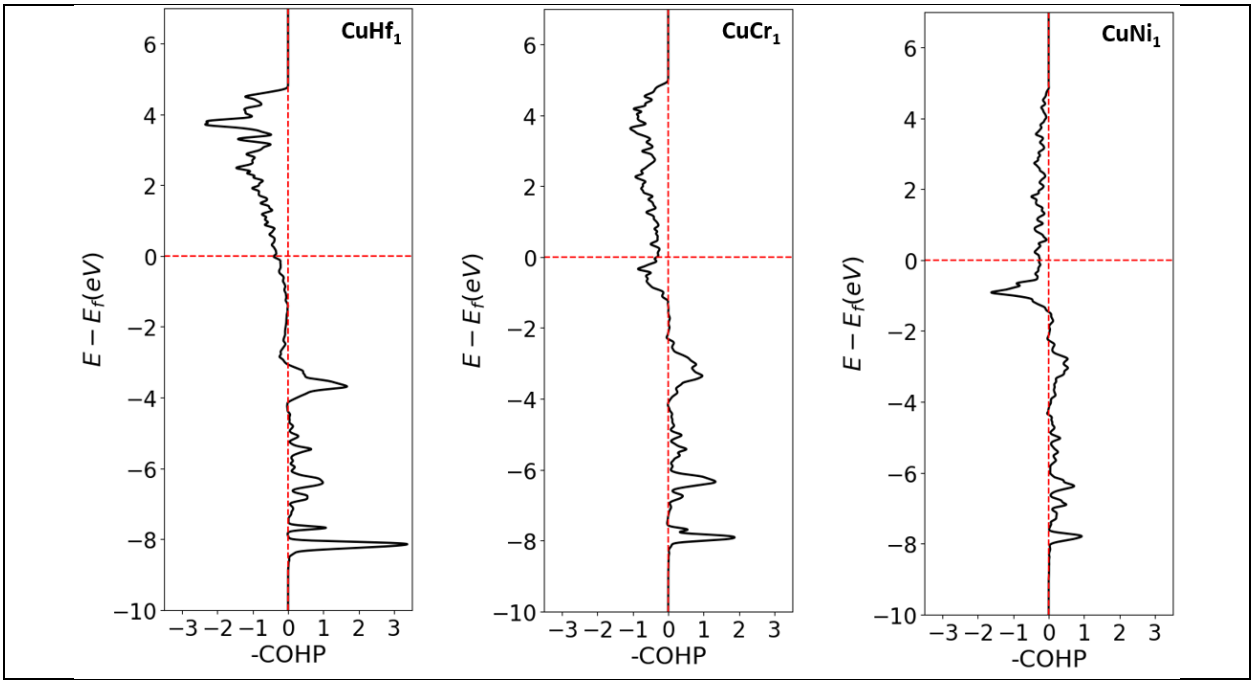

Figure 9. Crystal Orbital Hamilton Populations (COHP) curves of the interactions between the O atom in acrolein and the three different dopant elements in Cu(111): Hf, Cr, and Ni.

A Crystal Orbital Hamilton Populations (COHP) analysis was carried out to understand the differences between the early- (Hf), mid- (Cr), and late-transition metals (Ni) in Cu(111) from a chemical bond perspective (Figure 9). Specifically, this study focuses on the bonding strengths between the dopant atoms and the O atom in acrolein as they determine which adsorption configuration is more favorable. In the case of the late-transition metal, Ni, it is seen that a significant portion of the anti-bonding orbitals with positive COHP values is below the Fermi level. This large occupancy of the anti-bonding orbitals weakens the bonding between Ni and O, and helps explain the observation that C=O binding mode is not favored on $CuNi_1$. This claim is further supported by the small (absolute value-wise) integrated COHP value of -1.07 between the two atoms. Moving to the mid-transition metal, Cr, COHP analysis shows that a reduced portion of the anti-bonding orbitals are still populated when compared with Ni, as evidenced by both Figure 9 and its integrated COHP value of -2.72. The same trend persists when one progresses to the early-transition metal, Hf, which has an even smaller occupation of the anti-bonding orbitals and a greater integrated COHP value of -4.02. Not only are these results highly aligned with the C=O binding strengths observed earlier, they also demonstrate that the positions (relative to the Fermi level) of the anti-bonding orbitals between the dopants and the O atom in unsaturated aldehydes can be adjusted by dispersing different groups of transition metals in Cu(111). Hence, by carefully tuning its position, optimal reaction selectivity and reactivity could be attained simultaneously.

Prior to conclusion, it is important to note that an accurate description of the electronic structure requires to take into account the spin state on the dopant, and itself affected by the presence of the adsorbate. Among the three categories of transition metals, both early- and late-transition metals in Cu(111) are found to be non-magnetic, regardless of whether there is a surface intermediate on

top or not. Mid-transition metals of Cr and Mn in Cu(111), however, show magnetic moments, and these are preserved throughout the course of the reaction (Figure S10). Nevertheless, this study properly handles the spin states in the various systems investigated, and it sheds light on the promising catalysts (i.e. SAAs of mid-transition metals) for the selective hydrogenation of α,β-unsaturated aldehydes.

Conclusion:

Our theoretical study demonstrates the trend in Cu-based single-atom alloys for selective hydrogenation of α,β-unsaturated aldehydes to produce unsaturated alcohols. The segregation and aggregation energies of an ensemble of transition metals in Cu(111) were first calculated to evaluate the feasibility of making such catalysts in experiments. Out of these alloy combinations, early-transition metals Ti, Zr, and Hf, mid-transition metals Cr and Mn, and late-transition metals Rh, Ir, Ni, Pd, and Pt in Cu(111) are found to be realizable. The two different binding modes (i.e. C=O and C=C binding modes) of acrolein on these three categories of dopants were subsequently tested as a preliminary assessment of their selectivity for propenol formation. It is found that the early-transition metal atoms in Cu(111) strongly favor the C=O binding mode of the acrolein molecule, with the magnitude of the adsorption free energies being greater than 1.5 eV. This tight interaction between the surface species and the catalyst surface is also preserved for the mono-hydrogenated intermediates, which have free energy values lower than -2.00 eV. Although this feature seems to be tempting as it could stabilize the transition states for bond formation, it is too strong such that subsequent hydrogenation and desorption steps are highly endergonic in nature. Hence, acrolein hydrogenation cannot proceed on this type of SAAs.

Mid-transition metal atoms in Cu(111) are found to be the most promising for selective acrolein hydrogenation. These metals favor the C=O binding mode over the C=C binding mode, and the binding strength is moderate. DFT calculations and microkinetic modeling demonstrate that the selectivity for propenol formation on $CuCr_1$ is controlled by three elementary steps: (1) acrolein migration from the more stable C=O binding mode to the less stable C=C binding mode, (2) H-migration to the C=C binding acrolein and (3) O-H bond formation from the mono-hydrogenated intermediate. To help enhance the selectivity, high H_2 pressure is required as it can lower down the free energies of the steps that involve the introduction of more H atoms on the catalyst surface (e.g. O-H bond formation step), while the acrolein diffusion step remains unaffected and the H-migration step less impacted. It should be highlighted that the intrinsic errors in DFT calculations could have an impact on the computed selectivity. Hence, one could only suggest that it is highly likely that selective acrolein hydrogenation could be carried out on $CuCr_1$. The same could also apply to another mid-transition metal Mn, and they should be the first systems to be tested in experiments.

Lastly, late-transition metals in Cu(111) are unlikely to hydrogenate acrolein selectively. These metals favor the C=C binding mode over the C=O binding mode, and hence molecular migration is not required to produce the undesired product propanal. In addition, the transition states for propenol formation are found to be higher than those for propanal formation on $CuNi_1$, which is the late-transition metal that has the smallest energy difference between the two different binding modes of acrolein. This result shows that acrolein cannot be selectively hydrogenated on $CuNi_1$,

let alone other late-transition metals which possess even greater energy differences between the two binding modes. Nevertheless, unsaturated aldehydes with substituents attached to the C=C bond might possess higher selectivity as the presence of the substituents could destabilize the transition states in C=C bond hydrogenation and facilitate the desorption of the unsaturated alcohols.

The results underline that the simple descriptor of a favored C=O adsorption mode of the unsaturated aldehyde is contributing but not sufficient to ensure a high selectivity towards unsaturated alcohols. Rather, the magnitude of the migration barrier between the two binding modes also plays a crucial role in preventing access to the generally more reactive hydrogenation of the C=C bond. The trends presented in this study offer important insights into the properties that a specific single-atom alloy catalyst should possess for the selective hydrogenation of various α,β-unsaturated aldehydes. Dilute alloy catalysts appear as a versatile platform to tune the binding strength of intermediates and transition states, enabling a control of catalytic activity and selectivity.

Supporting Information. Details of microkinetic modeling, additional energy profiles and the corresponding adsorption configurations, surface coverage, degree of selectivity/rate control analysis, extra selectivity calculations and dopant magnetization.

Acknowledgments

This work was supported as part of the Integrated Mesoscale Architectures for Sustainable Catalysis (IMASC), an Energy Frontier Research Center funded by the U.S. Department of Energy, Office of Science, Basic Energy Sciences under Award No. DE-SC0012573. DFT calculations reported in this work used computational and storage resources on the Hoffman2 cluster at the UCLA Institute for Digital Research and Education (IDRE), the National Energy Research Scientific Computing Center (NERSC) of the U.S. Department of Energy, and the Bridges-2 cluster through the allocation CHE170060 at the Pittsburgh Supercomputing Center through ACCESS.

Reference:

(1) Dostert, K.-H.; O'Brien, C. P.; Ivars-Barceló, F.; Schauermann, S.; Freund, H.-J. Spectators Control Selectivity in Surface Chemistry: Acrolein Partial Hydrogenation Over Pd. *J. Am. Chem. Soc.* **2015**, *137* (42), 13496–13502.

(2) Mohr, C.; Claus, P. Hydrogenation Properties of Supported Nanosized Gold Particles. *Sci. Prog.* **2001**, *84* (4), 311–334.

(3) Marinelli, T. B. L. W.; Nabuurs, S.; Ponec, V. Activity and Selectivity in the Reactions of Substituted α,β-Unsaturated Aldehydes. *J. Catal.* **1995**, *151* (2), 431–438.

(4) Hoang-Van, C.; Zegaoui, O. Studies of High Surface Area Pt/MoO3 and Pt/WO3 Catalysts for Selective Hydrogenation Reactions. II. Reactions of Acrolein and Allyl Alcohol. *Appl. Catal. A Gen.* **1997**, *164* (1–2), 91–103.

(5) Győrffy, N.; Paál, Z. Acrolein Hydrogenation on PdPt Powder Catalysts Prepared by Colloid Synthesis. *J. Mol. Catal. A Chem.* **2008**, *295* (1–2), 24–28.

(6) Loffreda, D.; Delbecq, F.; Vigné, F.; Sautet, P. Chemo−Regioselectivity in Heterogeneous Catalysis: Competitive Routes for CO and CC Hydrogenations from a Theoretical Approach. *J. Am. Chem. Soc.* **2006**, *128* (4), 1316–1323.

(7) Laref, S.; Delbecq, F.; Loffreda, D. Theoretical Elucidation of the Selectivity Changes for the Hydrogenation of Unsaturated Aldehydes on Pt(111). *J. Catal.* **2009**, *265* (1), 35–42.

(8) Reyes, P.; Aguirre, M. .; Fierro, J. L. .; Santori, G.; Ferretti, O. Hydrogenation of Crotonaldehyde on Rh-Sn/SiO2 Catalysts Prepared by Reaction of Tetrabutyltin on Prereduced Rh/SiO2 Precursors. *J. Mol. Catal. A Chem.* **2002**, *184* (1–2), 431–441.

(9) Zhao, J.; NI, J.; Xu, J.; Xu, J.; Cen, J.; Li, X. Ir Promotion of TiO2 Supported Au Catalysts for Selective Hydrogenation of Cinnamaldehyde. *Catal. Commun.* **2014**, *54*, 72–76.

(10) Cao, Y.; Chen, B.; Guerrero-Sánchez, J.; Lee, I.; Zhou, X.; Takeuchi, N.; Zaera, F. Controlling Selectivity in Unsaturated Aldehyde Hydrogenation Using Single-Site Alloy Catalysts. *ACS Catal.* **2019**, *9* (10), 9150–9157.

(11) Aich, P.; Wei, H.; Basan, B.; Kropf, A. J.; Schweitzer, N. M.; Marshall, C. L.; Miller, J. T.; Meyer, R. Single-Atom Alloy Pd–Ag Catalyst for Selective Hydrogenation of Acrolein. *J. Phys. Chem. C* **2015**, *119* (32), 18140–18148.

(12) Luneau, M.; Lim, J. S.; Patel, D. A.; Sykes, E. C. H.; Friend, C. M.; Sautet, P. Guidelines to Achieving High Selectivity for the Hydrogenation of α,β-Unsaturated Aldehydes with Bimetallic and Dilute Alloy Catalysts: A Review. *Chem. Rev.* **2020**, *120* (23), 12834–12872.

(13) Hannagan, R. T.; Giannakakis, G.; Flytzani-Stephanopoulos, M.; Sykes, E. C. H. Single-Atom Alloy Catalysis. *Chem. Rev.* **2020**, acs.chemrev.0c00078.

(14) Han, J.; Lu, J.; Wang, M.; Wang, Y.; Wang, F. Single Atom Alloy Preparation and Applications in Heterogeneous Catalysis. *Chinese J. Chem.* **2019**, *37* (9), 977–988.

(15) Giannakakis, G.; Flytzani-Stephanopoulos, M.; Sykes, E. C. H. Single-Atom Alloys as a Reductionist Approach to the Rational Design of Heterogeneous Catalysts. *Acc. Chem. Res.* **2019**, *52* (1), 237–247.

(16) Darby, M. T.; Stamatakis, M.; Michaelides, A.; Sykes, E. C. H. Lonely Atoms with Special Gifts: Breaking Linear Scaling Relationships in Heterogeneous Catalysis with Single-Atom Alloys. *J. Phys. Chem. Lett.* **2018**, *9* (18), 5636–5646.

(17) Spivey, T. D.; Holewinski, A. Selective Interactions between Free-Atom-like d-States in Single-Atom Alloy Catalysts and Near-Frontier Molecular Orbitals. *J. Am. Chem. Soc.* **2021**, *143* (31), 11897–11902.

(18) Lee, J. D.; Miller, J. B.; Shneidman, A. V.; Sun, L.; Weaver, J. F.; Aizenberg, J.; Biener, J.; Boscoboinik, J. A.; Foucher, A. C.; Frenkel, A. I.; van der Hoeven, J. E. S.; Kozinsky, B.; Marcella, N.; Montemore, M. M.; Ngan, H. T.; O'Connor, C. R.; Owen, C. J.; Stacchiola, D. J.; Stach, E. A.; Madix, R. J.; Sautet, P.; Friend, C. M. Dilute Alloys Based on Au, Ag, or Cu for Efficient Catalysis: From Synthesis to Active Sites. *Chem. Rev.* **2022**, *122* (9), 8758–8808.

(19) Thirumalai, H.; Kitchin, J. R. Investigating the Reactivity of Single Atom Alloys Using Density Functional Theory. *Top. Catal.* **2018**, *61* (5–6), 462–474.

(20) Greiner, M. T.; Jones, T. E.; Beeg, S.; Zwiener, L.; Scherzer, M.; Girgsdies, F.; Piccinin, S.; Armbrüster, M.; Knop-Gericke, A.; Schlögl, R. Free-Atom-like d States in Single-Atom Alloy Catalysts. *Nat. Chem.* **2018**, *10* (10), 1008–1015.

(21) Ngan, H. T.; Yan, G.; van der Hoeven, J. E. S.; Madix, R. J.; Friend, C. M.; Sautet, P. Hydrogen Dissociation Controls 1-Hexyne Selective Hydrogenation on Dilute Pd-in-Au Catalysts. *ACS Catal.* **2022**, *12* (21), 13321–13333.

(22) Luneau, M.; Shirman, T.; Foucher, A. C.; Duanmu, K.; Verbart, D. M. A.; Sautet, P.; Stach, E. A.; Aizenberg, J.; Madix, R. J.; Friend, C. M. Achieving High Selectivity for Alkyne Hydrogenation at High Conversions with Compositionally Optimized PdAu Nanoparticle Catalysts in Raspberry Colloid-Templated SiO2. *ACS Catal.* **2020**, *10* (1), 441–450.

(23) Muir, M.; Molina, D. L.; Islam, A.; Abdel-Rahman, M. K.; Trenary, M. Selective Hydrogenation of Acrolein on a Pd/Ag(111) Single-Atom Alloy Surface. *J. Phys. Chem. C* **2020**, *124* (44), 24271–24278.

(24) Delbecq, F.; Sautet, P. Influence of Sn Additives on the Selectivity of Hydrogenation of α-β-Unsaturated Aldehydes with Pt Catalysts: A Density Functional Study of Molecular Adsorption. *J. Catal.* **2003**, *220* (1), 115–126.

(25) Zhou, C.; Ngan, H. T.; Lim, J. S.; Darbari, Z.; Lewandowski, A.; Stacchiola, D. J.; Kozinsky, B.; Sautet, P.; Boscoboinik, J. A. Dynamical Study of Adsorbate-Induced Restructuring Kinetics in Bimetallic Catalysts Using the PdAu(111) Model System. *J. Am. Chem. Soc.* **2022**, *144* (33), 15132–15142.

(26) Kresse, G.; Hafner, J. Ab Initio Molecular Dynamics for Liquid Metals. *Phys. Rev. B* **1993**, *47* (1), 558–561.

(27) Kresse, G.; Hafner, J. Ab Initio Molecular-Dynamics Simulation of the Liquid-Metalamorphous- Semiconductor Transition in Germanium. *Phys. Rev. B* **1994**, *49* (20), 14251–14269.

(28) Monkhorst, H. J.; Pack, J. D. Special Points for Brillouin-Zone Integrations. *Phys. Rev. B - Condens. Matter Mater. Phys.* **1976**, *13*, 5188–5192.

(29) Steinmann, S. N.; Corminboeuf, C. Comprehensive Benchmarking of a Density-Dependent Dispersion Correction. *J. Chem. Theory Comput.* **2011**, *7* (11), 3567–3577.

(30) Perdew, J. P.; Burke, K.; Ernzerhof, M. Generalized Gradient Approximation Made Simple. *Phys. Rev. Lett.* **1996**, *77* (18), 3865–3868.

(31) Methfessel, M.; Paxton, A. T. High-Precision Sampling for Brillouin-Zone Integration in Metals. *Phys. Rev. B* **1989**, *40* (6), 3616–3621.

(32) Blöchl, P. E. Projector Augmented-Wave Method. *Phys. Rev. B* **1994**, *50* (24), 17953–17979.

(33) Joubert, D. From Ultrasoft Pseudopotentials to the Projector Augmented-Wave Method. *Phys. Rev. B - Condens. Matter Mater. Phys.* **1999**, *59* (3), 1758–1775.

(34) Henkelman, G.; Jónsson, H. Improved Tangent Estimate in the Nudged Elastic Band Method for Finding Minimum Energy Paths and Saddle Points. *J. Chem. Phys.* **2000**, *113* (22), 9978–9985.

(35) Henkelman, G.; Uberuaga, B. P.; Jónsson, H. Climbing Image Nudged Elastic Band Method for Finding Saddle Points and Minimum Energy Paths. *J. Chem. Phys.* **2000**, *113* (22), 9901-9904.

(36) Henkelman, G.; Jónsson, H. A Dimer Method for Finding Saddle Points on High Dimensional Potential Surfaces Using Only First Derivatives. *J. Chem. Phys.* **1999**, *111* (15), 7010–7022.

(37) Maintz, S.; Deringer, V. L.; Tchougréeff, A. L.; Dronskowski, R. LOBSTER: A Tool to Extract Chemical Bonding from Plane-Wave Based DFT. *J. Comput. Chem.* **2016**, *37* (11), 1030–1035.

(38) Momma, K.; Izumi, F. VESTA 3 for Three-Dimensional Visualization of Crystal, Volumetric and Morphology Data. *J. Appl. Crystallogr.* **2011**, *44*, 1272-1276.

(39) Gokhale, A. A.; Kandoi, S.; Greeley, J. P.; Mavrikakis, M.; Dumesic, J. A. Molecular-Level Descriptions of Surface Chemistry in Kinetic Models Using Density Functional Theory. *Chem. Eng. Sci.* **2004**, *59* (22–23), 4679–4691.

(40) Campbell, C. T. The Degree of Rate Control: A Powerful Tool for Catalysis Research. *ACS Catal.* **2017**, *7* (4), 2770–2779.

(41) Shi, J.; Owen, C. J.; Ngan, H. T.; Qin, S.; Mehar, V.; Sautet, P.; Weaver, J. F. Formation of a Ti–Cu(111) Single Atom Alloy: Structure and CO Binding. *J. Chem. Phys.* **2021**, *154* (23), 234703.

(42) Lee, J. D.; Qi, Z.; Foucher, A. C.; Ngan, H. T.; Dennis, K.; Cui, J.; Sadykov, I. I.;

Crumlin, E. J.; Sautet, P.; Stach, E. A.; Friend, C. M.; Madix, R. J.; Biener, J. Facilitating Hydrogen Dissociation over Dilute Nanoporous Ti–Cu Catalysts. *J. Am. Chem. Soc.* **2022**, *144* (37), 16778-16791.

(43) Patel, D. A.; Giannakakis, G.; Yan, G.; Ngan, H. T.; Yu, P.; Hannagan, R. T.; Kress, P. L.; Shan, J.; Deshlahra, P.; Sautet, P.; Sykes, E. C. H. Mechanistic Insights into Nonoxidative Ethanol Dehydrogenation on NiCu Single-Atom Alloys. *ACS Catal.* **2023**, *13* (7), 4290–4303.

(44) Gautier, S.; Steinmann, S. N.; Michel, C.; Fleurat-Lessard, P.; Sautet, P. Molecular Adsorption at Pt(111). How Accurate Are DFT Functionals? *Phys. Chem. Chem. Phys.* **2015**, *17* (43), 28921–28930.

TOC Figure

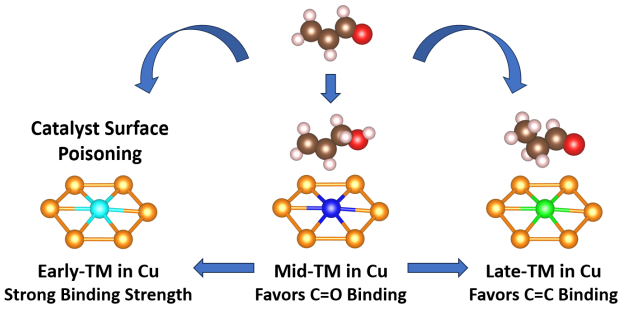
Catalyst Surface
Poisoning
Early-TM in Cu
Strong Binding Strength
Mid-TM in Cu
Favors C=O Binding
Late-TM in Cu
Favors C=C Binding